DOI: 10.1534/genetics.106.064360

Transposition of a Fungal Miniature Inverted-Repeat Transposable Element Through the Action of a *Tc1*-Like Transposase

Marie Dufresne,*[,1] Aurélie Hua-Van,[†,1] Hala Abd el Wahab,* Sarrah Ben M'Barek,[‡] Christelle Vasnier,* Laure Teysset,[§] Gert H. J. Kema[‡] and Marie-Josée Daboussi*[,2]

**Institut de Génétique et Microbiologie, Université Paris-Sud, UMR8621, F-91405 Orsay, France, [†]Laboratoire Evolution, Génomes et Spéciation, Centre National de la Recherche Scientifique, FR-91198 Gif-sur-Yvette, France, [‡]Wageningen University and Research Center, Plant Research International B.V., 6700 AA Wageningen, The Netherlands and [§]Institut Jacques Monod, Universités Paris 6 et 7, UMR7592, 75251 Paris, France*

Manuscript received August 4, 2006
Accepted for publication October 22, 2006

ABSTRACT

The *mimp1* element previously identified in the ascomycete fungus *Fusarium oxysporum* has hallmarks of miniature inverted-repeat transposable elements (MITEs): short size, terminal inverted repeats (TIRs), structural homogeneity, and a stable secondary structure. Since *mimp1* has no coding capacity, its mobilization requires a transposase-encoding element. On the basis of the similarity of TIRs and target-site preference with the autonomous Tc1-like element *impala*, together with a correlated distribution of both elements among the Fusarium genus, we investigated the ability of *mimp1* to jump upon expression of the *impala* transposase provided in *trans*. Under these conditions, we present evidence that *mimp1* transposes by a cut-and-paste mechanism into TA dinucleotides, which are duplicated upon insertion. Our results also show that *mimp1* reinserts very frequently in genic regions for at least one-third of the cases. We also show that the *mimp1/impala* double-component system is fully functional in the heterologous species *F. graminearum*, allowing the development of a highly efficient tool for gene tagging in filamentous fungi.

MINIATURE inverted-repeat transposable elements (MITEs) are a particular group of transposable elements (TEs), first described in plants (Bureau and Wessler 1992, 1994b; Casacuberta *et al.* 1998; Zhang *et al.* 2000, 2001; Santiago *et al.* 2002), but later found in a wide range of organisms including *Caenorhabditis elegans* (Oosumi *et al.* 1996), mosquitoes (Tu 1997, 2001; Feschotte and Mouches 2000), zebrafish (Plasterk *et al.* 1999), humans (Smit and Riggs 1996), and fungi (Yeadon and Catcheside 1995). MITEs share common structural features: the presence of terminal inverted repeats (TIRs), a small size (usually <600 bp), and no coding region. While they resemble previously characterized nonautonomous DNA elements, such as *Ds* (reviewed in Kunze and Weil 2002), the first MITEs identified in plants, *Tourist* and *Stowaway*, displayed other specific features: a stable secondary structure, AT richness, particular target-site duplications (TSD), a high copy number, and a great uniformity of size and sequence. However, as new miniature elements were identified, some exceptions were observed: GC-rich elements (Tu 2001), lack of secondary structure (Bureau *et al.* 1996), or moderate copy number (Holyoake and Kidwell 2003), suggesting that only some characteristics are shared by all MITEs.

More recently, a link between MITE families and well-characterized DNA transposons, belonging mainly to the Tc1-*mariner* superfamily (Feschotte *et al.* 2002), has been established on the basis of TIRs and TSD sequence similarities, supporting the idea that MITEs are a particular type of nonautonomous class II transposons. However, the origin of these short elements is still unclear: some exhibiting extended regions of similarity with full-length elements may have originated by internal deletions; others with homology limited to the TIRs or to terminal regions may originate *de novo* by capture of DNA sequences between the TIRs.

The classification of MITEs within class II TEs also implies that they are mobilized by a transposase from autonomous members of their own (or a related) family by a cut-and-paste mechanism. The recent studies on a rice MITE (Jiang *et al.* 2003; Kikuchi *et al.* 2003) confirmed the cut-and-paste mechanism and indicated that amplification could be influenced by specific (environmental or genomic) conditions (Jiang *et al.* 2003; Shan *et al.* 2005). However, although putative autonomous partners have been proposed for several MITE families, a clear demonstration that they are indeed necessary for MITE transposition is still lacking.

In *Fusarium oxysporum*, numerous DNA transposon families have been identified, mainly by trapping into a target gene or sequencing of some genomic regions

[1]These authors contributed equally to this work.

[2]*Corresponding author:* Institut de Génétique et Microbiologie, Bât 400, Université Paris-Sud, F-91405 Orsay Cedex, France.
E-mail: marie-jose.daboussi@igmors.u-psud.fr

(Daboussi and Langin 1994; Hua-Van *et al.* 2000; Daboussi and Capy 2003). Autonomous members of the Tc1-*mariner* superfamily have been identified: *Fot1* is a *pogo*-like element that may be present in a relatively high copy number (~100 copies), essentially full-length copies (Daboussi *et al.* 1992; Migheli *et al.* 1999); *impala* is a representative of the Tc1 family (Robertson 2002) present in low copy number and composed of at least five different subfamilies (E, D, F, K, and P) (Hua-Van *et al.* 2001a). Two of these (E and D) contain autonomous members presenting up to 20% divergence at the DNA level (Hua-Van *et al.* 1998, 2001b). By sequencing genomic regions surrounding copies of the *D* subfamily, five elements of ~200 bp were identified. These elements, called *mimp*, have no coding capacity but display TIRs very similar to those of *impala* (Hua-Van *et al.* 2000). We wondered whether these short elements are mobile and, if so, whether they could be transactivated by an *impala* transposase. Here we show that the *mimp1* family is present in a number of related species and that its distribution follows the distribution of *impala*. Using a phenotypic excision assay in two different species, we demonstrate that they are *trans*-mobilized by the *impala* transposase and that transposition occurs through a cut-and-paste mechanism. The functionality of the double-component system in the heterologous species *F. graminearum*, the genome sequence of which is available, provided the opportunity to analyze the insertion site preference of newly transposed copies. Preliminary results suggest that this system is an interesting alternative tool for gene tagging in filamentous fungi.

MATERIALS AND METHODS

Fungal strains: *F. oxysporum* strains FOM150 *nia9* and FO5 *nia13* are nitrate-reductase-deficient mutants usually used as recipient strains in transformation experiments (Migheli *et al.* 1999; Hua-Van *et al.* 2001b). The *F. graminearum* strain Fg820 was kindly provided by G. H. J. Kema. Four nitrate-reductase mutants, named Fg820 *nia1*, Fg820 *nia5*, Fg820 *nia6*, and Fg820 *nia14*, were obtained as previously described and also used as recipient strains in transformation experiments. Strains belonging to the *F. oxysporum* complex (FO complex) and used in this study (FOM24, FOM150, FOM7, FOM466A, FOMP2, FO5, FO47, FOR4, FORL28, FOA1, FOLn3, FOVR1, FOVR3, FOD11, FOL15, and FOMK419) have been described in Hua-Van *et al.* (2001a). Strains from related species, *i.e.*, *F. foetens* (NRRL31852), *F. redolens* (NRRL25600 and 28381), and *F. hostae* (NRRL29642), were obtained from K. O'Donnell (National Center for Agricultural Utilization Research, U. S. Department of Agriculture, Peoria, IL). More distant species from the *Discolor* (*F. culmorum*) and *Martiella* (*F. caucasicum* and *Neocosmospora* sp.) sections have also been used (Daboussi *et al.* 2002).

Plasmids: pHEO62 contains the ORF encoding the *impalaE* transposase (Hua-Van *et al.* 1998), cloned between the *gpdA* promoter and the *trpC* terminator of *Aspergillus nidulans*. The entire cassette was extracted from plasmid pEO62 (Li Destri Nicosia *et al.* 2001) as an *Eco*RI/*Hin*dIII fragment and cloned into plasmid pBC1004 (Carroll *et al.* 1994), which permits hygromycin selection. pNm1H18 was constructed by introduction of a *mimp1* element into the first intron of the *niaD* gene (Figure 3). This *mimp1* copy corresponds to the reamplification of the *mimp1.1* element (AF076624) using the HindImp primer (5′-GCCCTAAGCTTACAGTGGGGTGCAA TAAGTTTG-3′). This primer anneals to the TIRs of *mimp1* and *impala* and contains a *Hin*dIII site (underlined) at the 5′-end. PCR conditions were 1 min denaturation at 95°, followed by 30 cycles of 1 min at 94°, 1 min at 59°, and 30 sec at 72°, and then an elongation step of 10 min at 72°. The PCR product was then digested with *Hin*dIII and inserted into the *Hin*dIII site of the first intron of the *niaD* gene in plasmid pAN301 (Malardier *et al.* 1989), deleted from a dispensable *Nde*I fragment (in which a *NdeI* fragment located downstream of the *niaD* gene has been removed), resulting in the *niaD::mimp1* construct.

Transformation experiments: The transformation procedure was as described (Hua-Van *et al.* 2001b). Plasmid pNm1H18 was introduced into strain FOM150 *nia9*, which contains different sources of transposases, including *impalaE* and *D* (Hua-Van *et al.* 2001b), together with plasmid pAN7-1 (Punt *et al.* 1987) carrying the selectable marker *hph* conferring resistance to hygromycin B. Plasmid pNm1H18 was also introduced in the FO5 *nia13*, Fg820 *nia1*, Fg820 *nia5*, Fg820 *nia6*, and Fg820 *nia14* strains, devoid of all types of TEs identified within the FO complex (Migheli *et al.* 1999; Hua-Van *et al.* 2001b; Chalvet *et al.* 2003), together with plasmid pAN7-1 or plasmid pHEO62, which carries the source of *impalaE* transposase together with the selectable marker *hph*. In all three genetic contexts, cotransformants containing plasmid pNm1H18 were identified among hygromycin-resistant transformants through colony hybridization, using a *niaD* probe from plasmid pAN301 (Malardier *et al.* 1989).

Revertant selection: Spores of cotransformants were recovered by washing and filtration from a single spore culture grown on solid medium and spread at different dilutions on nitrate minimal agar medium supplemented with triton X100 (0.06%) as previously described (Hua-Van *et al.* 2001b). Alternatively, plugs of each cotransformant were picked on plates of nitrate minimal agar medium. Revertants are easily detected as patches of aerial mycelium with a wild-type phenotype on a background of sparse mycelium corresponding to a *niaD* mutant (Figure 4).

DNA preparation and Southern blot analysis: DNA extractions from *F. oxysporum* strains were conducted as previously described (Langin *et al.* 1990). Extraction of genomic DNA from *F. graminearum* strains was performed using another procedure. Approximately 10^6 spores were spread on a cellophane disk onto a potato dextrose agar plate. After overnight growth at 26°, germlings were scraped and frozen in liquid nitrogen. After adding 600 μl of lysis solution (100 mM Tris pH 9.0, 10 mM EDTA, 1% sarkosyl) and ~100 μl of glass beads (200- to 500-μm diameter, Fisher Scientific, Illirch, France), the mycelium was ground using the Fastprep101 machine (twice for 30 sec at 4000 rpm). DNA was purified by successive extractions using phenol, phenol/chloroform (1/1), and chloroform and then precipitated by adding 1/20 vol 3 M sodium acetate and 0.6 vol isopropanol. After a washing step in 70% ethanol and drying, genomic DNA was resuspended in sterile distilled water plus RNAse A at a final concentration of 1 mg/ml and incubated 1 hr at 37° for RNA digestion. Ten micrograms of genomic DNA was digested with *Eco*RI or *Xba*I, separated electrophoretically on 0.7% agarose gels, and transferred on nylon membranes, using a vacuum blotter. DNA templates were ^{32}P-labeled using the *redi* primeII kit (Amersham Biosciences). Hybridizations were conducted under standard conditions (Sambrook *et al.* 1989).

Polymerase chain reaction and primer sequences: Hybridization probes were obtained by PCR. Primers SpeE3 and

SpeE5 (Hua-Van *et al.* 2001a) were used to generate a PCR product corresponding to *impala* elements of the E subfamily, with 50 ng of genomic DNA from the FOM24 strain as a template. PCR conditions were as described in Hua-Van *et al.* (2001a). The HindImp primer was used, as described above, to generate either PCR products from different genomic DNAs (see Figure 1D) or the *mimp1* PCR product used as a probe. The 419-bp *niaD* probe was generated with primers niaCG1 (5′-CACTAGTATGTGCAGGCAAC-3′) and niaCG2 (5′-TTCA GCCACTTGACACTG-3′), using the pAN301 plasmid as a template. PCR conditions were as follows: 2 min at 94°, then 30 cycles of 30 sec at 94°, 30 sec at 59°, and 2 min at 72°.

The size homogeneity of *mimp1* elements in the different Fusarium strains was determined using *mimp1*-specific primers: SPEmimp1-5′ (5′-*CAATAAGTTTGAATACC*GGGCGTG-3′) and SPEmimp1-3′ (5′-*GTTTGAATACC*TTTTGATTTG-3′), both with overlapping TIRs (italics) and with internal sequences (underlined). In reference to the full-length *mimp1.1* element previously identified (Hua-Van *et al.* 2000), the expected size of the PCR product is 197 bp. PCR conditions enabling the amplification of larger DNA molecules were used: a denaturation step of 1 min at 95° followed by 35 cycles of 1 min at 94°, 1 min at 53°, 2 min 30 sec at 72° and a final elongation step of 10 min at 72°.

mimp1 amplification in different strains was obtained using primer mi1 (5′-TACAGTGGGATGCAATAAGTTTGAATAC-3′) located within TIRs, alone or in combination with primers SacR (5′-CTGAGGAGGGAGCTCGATCTAGCC-3′) or SacF (5′-GGC TAGATCGAGCTCCCTCCTCAG-3′). A denaturation step of 3 min at 95° followed by 35 cycles of 30 sec at 95°, 30 sec at 59°, 1 min at 72°, and a final extension of 5 min at 72° was used.

Characterization of the FO5 endogenous *mimp1* copy was performed using the HindImp primer alone or in combination with SacR or SacF. PCR conditions were 5 min at 95° and then 45 cycles of 1 min at 94°, 1 min at 59°, and 1 min at 72° and a final elongation step of 10 min at 72°.

Excision events were controlled by PCR on 50 ng of genomic DNA of putative revertants and of the corresponding transformants, using primers niaD144 (5′-GTTCATGCCGTG GTCGCTGC-3′) and niaD754r (5′-AGTTGGGAATGTCCTCG TCG-3′) under the following conditions: 4 min at 94° and then 30 cycles of 1 min at 94°, 1 min at 59°, and 2 min at 72°. The sizes of the expected PCR products are 717 bp for a transformant and 485 bp for a revertant.

Amplification of *mimp1* flanking sequences: Two approaches were used to recover *mimp1* flanking sequences. For nonsequenced Fusarium strains, inverse PCR was performed. A 100-ng aliquot of genomic DNA of a given strain was digested with either one or two restriction enzymes at 37° during 30 min. The enzymes were then inactivated by incubation at 65° for 10 min. A total of 30 ng of the digested DNA was self-circularized during 30 min at room temperature using T4 DNA ligase (Biolabs) in a final volume of 10 μl. The ligase was then inactivated by incubation at 65° for 10 min. Approximately 7.5 ng of ligated DNA was used in PCR experiments with the primers Div149 (5′-GCAGGCTAAACTCCAAATAGGC-3′) and Div53 (5′-GTAGCGTGGCTCAAAGAGGC-3′), which correspond to internal regions of the canonical *mimp1* element and are directed toward the TIRs. The amplification program was as follows: a denaturation step of 1 min at 95° and then 1 min at 94°, 45 sec at 58°, and 4 min at 72° for 35 cycles, followed by an elongation step of 10 min at 72°.

For revertants from the *F. graminearum* genetic background, *mimp1* flanking sequences were recovered using a modified thermal asymetric interlaced (TAIL)–PCR approach. (Liu and Whittier 1995). Two rounds of PCR were performed on 50 ng of genomic DNA of the revertants. In the primary PCR, the arbitrary degenerate (AD) primer AD2, 5′-AG(A/T)GNAG(A/T) ANCA(A/T)AGA-3′, and the specific primer m1Div53F, 5′-GC CTCTTTGAGCCACGCTAC-3′, were used with reduced-stringency and high-stringency annealing temperatures of 44° and 66°, respectively. The secondary PCR was set up on 2 μl of a 1/100 dilution of the primary PCR, using the same AD primer and Div149 (see above) as the second specific primer. The annealing temperatures were the same as for the primary PCR. PCR programs were as described in Liu and Whittier (1995).

Cloning of PCR products and DNA sequencing: PCR products were directly cloned into the pGEM-T Easy vector (Promega, Madison, WI) using 3 μl of either rough or purified PCR products, following the manufacturer's instructions. Sequencing of PCR products cloned into the pGEM-T Easy vector was performed by Genome Express (Meylan, France) using an ABI Big Dye terminator kit (Perkin-Elmer, Norwalk, CT) and the universal M13/pUC sequencing primer (−20) (forward) and pR primer (5′-GGAAACAGCTATGACCATG-3′; reverse).

Sequence analysis: Multiple alignments were performed using Clustal W (Thompson *et al.* 1994) and slightly modified at both 5′- and 3′-ends for improvement. The parsimony analysis was realized on 179nt using PAUP4.0b10 (Swofford 2002) with default parameters. The bootstrap analysis comprised 100 replicates. The potential of the sequences to form stable secondary structures was analyzed with the RNAFOLD program (http:www.infobiogen.fr) using standard parameters. Searches for matches of nucleotide sequences in the current database (nonredundant GenBank) or in the *F. graminearum* Genome Database available at the Munich Information Center for Protein Sequences (MIPS) (http://mips.gsf.de/genre/proj/fusarium/) used the BlastN or BlastX algorithms (Altschul *et al.* 1997).

RESULTS

The *mimp1* MITE family: We previously described five copies of a putative MITE family, called *mimp*, discovered in the genome of *F. oxysporum* (strain FOM24) by sequencing genomic regions nested with TEs (Hua-Van *et al.* 2000). They are characterized by a small size (~220 bp), the lack of coding capacity, and the presence of short terminal inverted repeats of 27 bp (Figure 1A). They have been grouped into two subfamilies (*mimp1* and *mimp2*) on the basis of an absence of internal sequence homology. The *mimp* TIRs present a strong similarity with the first 27 nt of *impala* ends (Figure 1B), a *F. oxysporum* Tc1-like family organized in different subfamilies (Hua-Van *et al.* 1998, 2001b). Furthermore, *mimp* are flanked by TA dinucleotides, as is *impala*, which presumably correspond to the target duplication generated upon integration. Apart from the TIRs, no obvious sequence similarities were found between *mimp* and *impala*, or between *mimp* and any other known repetitive element.

To gain insight into the structure and the evolution of the *mimp1* family, we used a PCR approach to investigate sequence and size variability of *mimp1* elements in different genetic contexts belonging to the Fusarium genus. Primers located in the TIRs were first used and allowed amplification of fragments of different sizes in several strains. It was then determined that the larger ones (>220 bp) corresponded to full-length (1300 bp) or internally deleted (400–600 bp) *impala* (Figure 1C,

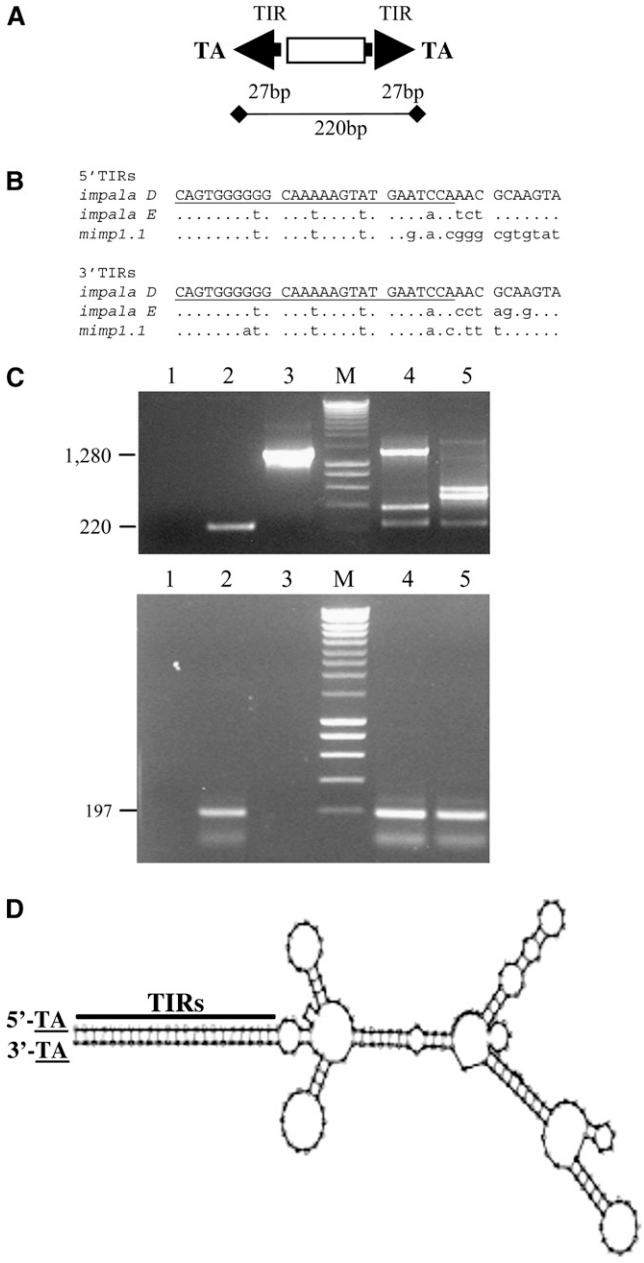

FIGURE 1.—(A) *mimp1* structure. (B) Sequence comparison of TIRs between *impala* elements and the *mimp1.1* copy. Dots indicate sequences that are identical to the *impala D* TIRs sequence (37 bp). Lowercase letters indicate sequence variation. *mimp1* and *impala* TIRs align over the first 27 nucleotides (underlined in the *impala D* sequences). (C) Agarose gel electrophoresis of PCR products obtained from two different *F. oxysporum* strains. Genomic DNAs of FOM24 (lane 4) and FOL15 (lane 5) were amplified using either the HindImp primer specific for TIRs (top) or for the *mimp1*-specific primers (bottom; see MATERIALS AND METHODS). Lanes 1–3 correspond to controls: 1, no DNA control; 2, pNm1H18 plasmid carrying the *mimp1.1* copy; 3, pNI160 plasmid carrying *impala160* (HUA-VAN *et al.* 2001b). Lanes labeled as M were loaded with a molecular weight marker (SmartLadder, Eurogentec). (D) Predicted secondary structure of the *mimp1* element, using the RNAFOLD program (http://www.infobiogen.fr).

top, lanes 4 and 5) while the 220-bp product was *mimp1* amplicon. In contrast, the use of *mimp1*-specific primers (see MATERIALS AND METHODS) under the same conditions each time revealed only the expected 197-bp PCR product (Figure 1C, bottom).

In addition to the uniformity in size of the different amplified full-length copies, the *mimp1* family also contains some truncated elements at either the 5′- or the 3′-end. Indeed, three truncated copies were previously identified (HUA-VAN *et al.* 2000). In this analysis, we obtained one other truncated copy among 18 independent inverse-PCR products recovered from different species (data not shown).

A total of 37 new *mimp1* sequences were obtained either by sequencing of FOM24 genomic clones (6) or by PCR (31) for other strains, including 12 from various strains of *F. oxysporum* and 19 from other closely related species. The latter ones were obtained using a combination of specific internal and TIR primers. These sequences corresponded to 23 different nucleotide sequences that were aligned with the four known *mimp1* sequences and a sequence retrieved from the GenBank database (AJ608703). The nucleotide differences calculated on 179 internal nucleotides (excluding the primer sequences) ranged from 0 to 20% within species as well as between species. This relatively high sequence identity has allowed us to perform a conventional phylogenetic analysis. A tree deduced from this alignment permits us to define clearly only one well-supported clade, containing sequences closely related mainly from FOM24. Others were more scattered and did not show clustering according to the species (data not shown).

Finally, the *mimp1* nucleotide sequence showed a strong potential to form a stable secondary structure (see Figure 1D). Although some exceptions exist (BUREAU *et al.* 1996), a number of MITE elements display this property. The *mimp1* predicted a ΔG_0 value of −87.7 kcal/mol that corresponds to the lowest values reported for other families (BUREAU and WESSLER 1994a; CASACUBERTA *et al.* 1998).

In conclusion, the *mimp1* elements showed an inverted terminal repeated structure that was able to fold into a stable secondary structure. The family appears homogeneous in size, in contrast with most nonautonomous elements such as internally deleted *impala*. The sequence of the TIRs (similar to those of *impala*) and of the TSD indicated a relationship with the Tc1-*mariner* superfamily of class II transposons, a group known to be associated with numerous MITE families (FESCHOTTE *et al.* 2002).

Copy number and genomic representation in the Fusarium genus: We first examined *mimp1* distribution in a wide collection of strains of the Fusarium *oxysporum* complex (FOC), previously studied for the presence of different TEs (HUA-VAN *et al.* 2001a; DABOUSSI *et al.* 2002; CHALVET *et al.* 2003). This analysis was extended to different *Fusarium* species either phylogenetically

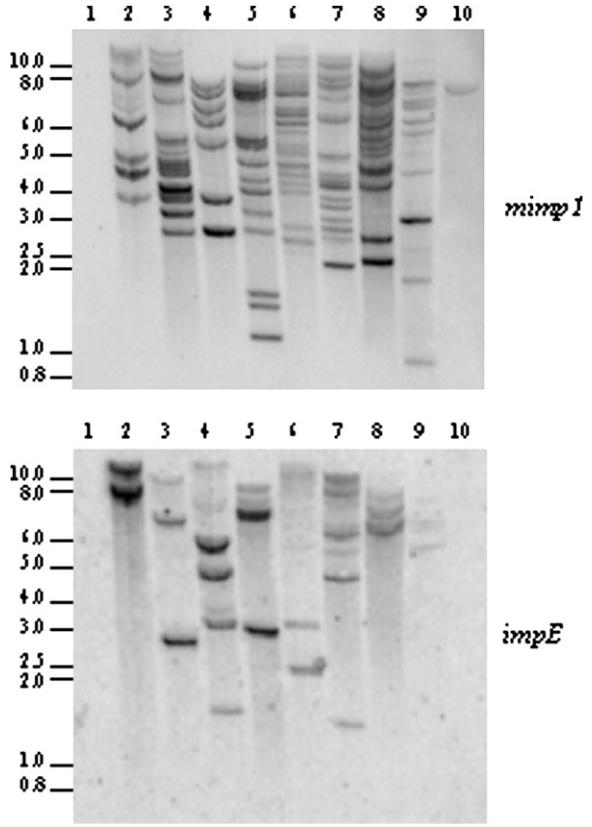

FIGURE 2.—Distribution of *mimp1* and *impala* elements in the genome of Fusarium strains. Genomic DNAs were digested by *Eco*RI and probed with the *mimp1* element or the *impala E* amplification product under high-stringency conditions. 1, *F. culmorum* strain 1602; 2, *F. foetens* strain 31852; 3, *F. redolens* strain 29642; 4, *F. hostae* strain 28381; 5, FOr4; 6, FOa1; 7, FOLn3; 8, FOL15; 9, FOM K419; 10, FO5.

closely related to FOC (BAAYEN *et al.* 2001; SKOVGAARD *et al.* 2003) or more distantly related.

Southern blot experiments performed on 16 FOC strains, representative of seven formae speciales and one nonpathogenic strain, revealed that all contained *mimp1* elements (Figure 2; data not shown). *mimp1* was also detected in the three strains from FOC-related species (Figure 2, lanes 2–4), but not in more distant species (Figure 2, lane 1; data not shown).

When detected, *mimp1* appears to be repetitive. The copy number varied between 7 and 20, according to the number of hybridizing bands observed in the Southern blot (Figure 2). It is noteworthy that some hybridizing bands present a signal of stronger intensity, which could result either from the presence of several *mimp* copies on the same fragment or from a difference in the size of the *mimp1* copy—full-length *vs.* truncated. Alternatively, weaker signals could result from nucleotide divergence preventing strong hybridization, as previously observed for the different *impala* subfamilies (HUA-VAN *et al.* 1998, 2001b).

The TIR similarity of *mimp1* and *impala* elements suggests that *mimp1* could use the *impala* transposase to move and multiply. To clarify the functional relationship between *mimp1* and *impala*, the presence of *impala*, the putative autonomous partner of *mimp1*, was also investigated in these genomes. The membranes used to detect *mimp1* were thus hybridized with an *impala* probe allowing the detection of the *impala E* subfamily (see MATERIALS AND METHODS). As observed for *mimp1*, the distant species appeared to be devoid of *impala*. In all the strains containing *mimp1* elements, *impala* signals were observed except in FO5 (Figure 2, lane 10). Beyond the absence of *impala* signal, this context was already shown to lack any *impala* activity (HUA-VAN *et al.* 2001b). We attempted to explain the unique faint *mimp1* hybridization signal by conducting PCR experiments. No amplification was obtained using specific TIR primers, even with extended elongation time. Using a combination of specific internal and TIR primers, only the 3′ part could be amplified (data not shown), indicating that the *mimp1*-hybridizing band in FO5 likely corresponds to a truncated copy. Moreover, the corresponding sequence showed only one nucleotide difference with the *mimp1* consensus sequence (>59 positions). The weakness of the hybridization signal in FO5 could thus reflect the truncation of this copy rather than a high sequence divergence.

Hence, *mimp1* and *impala* seem to exhibit a similar distribution within the Fusarium genus except in the FO5 strain.

Mobilization of *mimp1* by an autonomous *impala* element: Given TIR and target-site similarities between *mimp1* and *impala*, as well as the presence of *mimp1* in strains containing *impala* elements, it was tempting to speculate that the nonautonomous *mimp1* elements could be mobilized by the transposase encoded by an autonomous *impala* element (MIGHELI *et al.* 1999; HUA-VAN *et al.* 2001b; CHALVET *et al.* 2003). To test this hypothesis, we performed a phenotypic assay for excision, previously used to demonstrate transposition of different TEs (MIGHELI *et al.* 1999; HUA-VAN *et al.* 2001b; CHALVET *et al.* 2003). To this end, we constructed a plasmid, pNm1H18, in which a *mimp1* element was inserted within the first intron of the *niaD* gene, leading to a nonfunctional gene (see MATERIALS AND METHODS and Figure 3). This construct was introduced in three genetic backgrounds, which contained or lacked an *impala* source of transposase. The strain FOM150 *nia9* contains different autonomous *impala* copies, and this context has been already used to verify the mobility of defective *impala* copies (HUA-VAN *et al.* 2001b). Three [*nia*$^-$] transformants carrying pNm1H18 yielded Nia$^+$ revertant colonies (1–5/plate). Southern blot and PCR analyses performed on a sample of Nia$^+$ colonies revealed that *mimp1* is mobile and has been excised from *niaD* (data not shown). The excision events were confirmed by the presence of excision footprints at the empty sites (Table 1). The FO5 *nia13* context is devoid of all types of TEs previously identified within the FO complex (MIGHELI *et al.* 1999; HUA-VAN *et al.* 2001b;

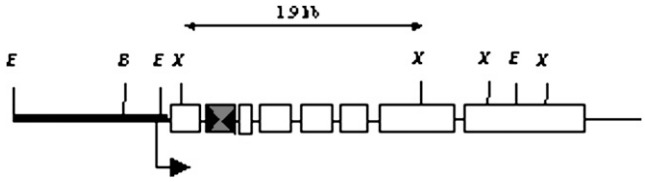

Figure 3.—Structure of plasmid pNm1H18 used for the phenotypic assay for excision. The 1.3-kb -*niaD* promoter is indicated as a thick line. *niaD* exons are shown as open rectangles. *mimp1* is the shaded rectangle in which large arrowheads represent TIRs. Restriction enzyme sites are indicated as E, *Eco*RI; B, *Bam*HI; X, *Xba*I.

Chalvet *et al.* 2003). From seven transformants in which pNm1H18 was introduced alone, very few Nia$^+$ colonies were observed (<1 colony/plate). Of the three recovered, only one showed an empty site, but sequencing revealed a 5-nt deletion instead of a typical footprint of two to five additional nucleotides (Table 1); the two others still showed the *mimp1* copy into the *niaD* intron. When plasmid pNm1H18 was introduced into the same genetic background, together with the plasmid carrying the *impalaE* transposase under the control of a strong promoter, we obtained 6 cotransformants, 5 of them giving numerous Nia$^+$ colonies (5–50/plate, see Figure 4). The remaining cotransformant gave very few Nia$^+$ colonies, none of them resulting from *mimp1* excision but more likely from reversion of the endogenous *nia* gene, as previously observed (Migheli *et al.* 1999; Hua-Van *et al.* 2001b; Chalvet *et al.* 2003). In the *F. graminearum* genetic background, similar results were observed. A total of 11 transformants carrying the pNm1H18 alone were obtained. None of them gave rise to Nia$^+$ colonies even after 6 weeks of growth on nitrate minimal agar medium. On the contrary, among 41 cotransformants carrying the pNm1H18 plasmid, together with the pHEO62 plasmid carrying the exogenous source of *impala* transposase, 33 gave rise to Nia$^+$ colonies, the number varying from 4 to 20/petri dish (data not shown).

A molecular analysis of one FO5 *nia13* transformant (TR55) and a sample of its revertants indicated that this transformant contained a single intact copy of the *niaD::mimp1* construct on the basis of the shift of the *niaD*-hybridizing band from 1.9 kb (occupied site) in TR55 to 1.7 kb (empty site) in all the revertants (Figure 5A, middle). We also observed at least one copy of the plasmid carrying the transposase gene (Figure 5A, top).

TABLE 1

Results of molecular analyses performed on a sample of NiaD$^+$ colonies

Genetic context	Source of transposase	No. of NiaD$^+$ colonies analyzed[a]	Excision event	Footprint
FOM150 *nia9*	Endogenous	5 (3)	Yes	cagTA (4) ctgTA (1)
FO5 *nia13*	None	3 (2)	No[b]	—
	Exogenous	3 (1)	No[c]	—
		22 (5)	Yes	cagTA (11) ctgTA (9) caTA (1) TA (1)
Fg820*nia*	None	0	—	—
	Exogenous	12 (12)	Yes	cagTA (7) ctgTA (3) caTA (2)

mimp1 excision events were detected by PCR analysis using primers (niaD144 and niaD754r), allowing amplification of a 485-bp fragment corresponding to an empty site (excision event, yes) in the niaD$^+$ revertants instead of a 717-bp fragment in the transformant corresponding to the insertion site occupied by the *mimp1* element. Footprints are composed of nucleotides from the ends of *mimp1* (lowercase) and the TA duplicated target site.

[a] The numbers of transformants from which the NiaD$^+$ colonies were obtained are indicated in parentheses.

[b] One revertant carries an empty site; however, sequencing revealed a 5-nt deletion instead of a typical footprint.

[c] The NiaD$^+$ colonies recovered from this transformant, which do not show an empty site, likely result from a reversion of the mutation in the recipient strain since we demonstrated that the exogenous source of transposase had been disrupted.

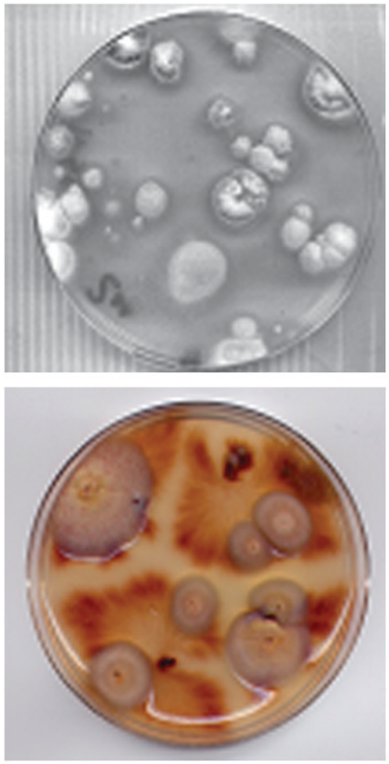

Figure 4.—Selection of excision events. The high number of niaD$^+$ colonies that can be selected from an FO5 (top) or a Fg820 (bottom) transformant carrying the *niaD::mimp* construct and an exogenous source of transposase. Plates were inoculated with 10^3 conidia or with four mycelia plugs and incubated for 1 month at 26°.

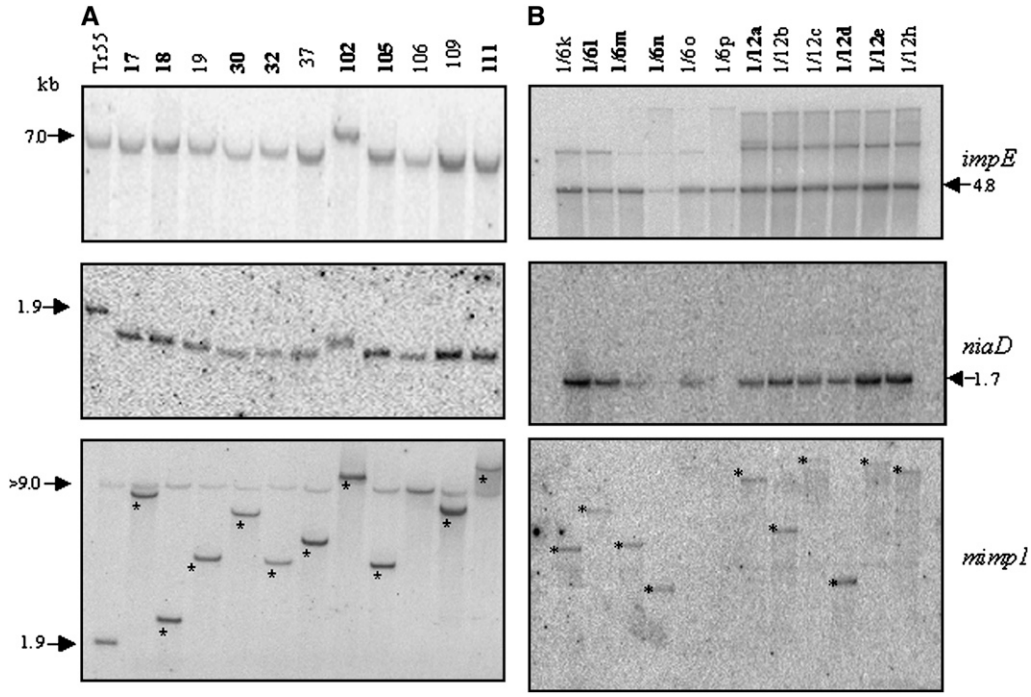

FIGURE 5.—Southern blot analysis of transformant TR55 and a sample of corresponding revertants in the FO5 genetic background (A) and of a sample of revertants obtained from two independent transformants in the Fg820 background (B). Genomic DNA was digested with *Xba*I and membranes were successively hybridized with an *impalaE* probe (top), a *niaD* probe (middle), and a *mimp1* probe (bottom). The stars indicate the reinsertion of excised copies. Numbers in boldface type correspond to revertants submitted to IPCR (FO5) or TAIL–PCR (Fg820).

The excision of *mimp1* was confirmed using a rapid PCR screen, which revealed, in each case, the presence of an excision footprint (Table 1). These footprints were very similar to those obtained in the *impala* active context (FOM150 *nia9*) and were also similar to those left by *impala* excision. Generally, five additional nucleotides were left, two corresponding to the duplicated TA target site and three from one of the ends of the element (HUA-VAN *et al.* 2001b).

The reinsertion of *mimp1* was assessed using a probe corresponding to the entire element (Figure 5A, bottom). A new hybridizing band, corresponding to a reinserted element, was observed in ~91% (10/11) of the revertants analyzed.

Similarly, the molecular analysis of 12 revertants derived from two independent cotransformants from the Fg820*nia* background was performed. Hybridization with the *impE* probe showed that each strain contains at least one intact copy of the construct carrying the source of transposase as shown by the presence of a 4.8-kb hybridizing *Xba*I fragment (Figure 5B, top). Additional bands were observed, corresponding most likely to a disrupted copy of the same plasmid. The presence of a single 1.7-kb hybridization band using the *niaD* probe demonstrated that all correspond to an excision event (Figure 5B, middle). Another set of 12 revertants, each derived from a different transformant, was used to examine the presence of excision footprints at the empty site. Typical excision footprints were found in all cases (Table 1). Using the *mimp1* element as a probe, reinsertion was observed in ~83% (10/12) of the strains analyzed. These results tend to confirm that the reinsertion frequency appears higher than that observed for *impala*, which is in the range of 50–75% (MIGHELI *et al.* 2000; HUA-VAN *et al.* 2001b).

Molecular analysis of *mimp1* insertion sites: Previous studies indicate that some MITE families insert preferentially into genic regions (MAO *et al.* 2000; ZHANG *et al.* 2000) and/or have a propensity to insert into each other, giving nested structures (JIANG and WESSLER 2001). In addition, for a given family, the distribution of ancient *vs.* recently inserted elements with respect to predicted genes can vary (SANTIAGO *et al.* 2002), suggesting that selection can also shape the genomic distribution of MITEs.

To obtain data on the target-site preference of *mimp1* elements, the regions flanking different *mimp1* elements were cloned by inverse polymerase chain reaction (IPCR) or TAIL–PCR, sequenced, and used to seek homologies in databases. For those giving a match, we calculated the distance to putative initiator ATGs or stop codons of the closest predicted genes. Two types of *mimp1* insertions were considered: (i) elements originally present in the genome of formae speciales of *F. oxysporum* or different Fusarium species closely related to the FOC and (ii) newly inserted elements either in the FO5 or in the Fg820 backgrounds, resulting from the mobilization of the *mimp1* copy by the *impala E* transposase, totaling 43 *mimp1*-insertion sites.

The four copies of *mimp1* previously identified in FOM24 (*mimp1.1-mimp1-4*) had been found in transposon nests (HUA-VAN *et al.* 2000). From 18 other ancient insertions analyzed, 10 clones yielded no significant hits in the databases, 7 showed high homology with known transposable elements (Table 2), and 1 corresponded to the insertion of *mimp1* in the 5′-untranslated region of a fungal gene, very close to the putative start

TABLE 2

Insertion sites of resident or newly reinserted *mimp1* elements

Clone	IPCR product size (sequenced)	Major BLAST hits	*e*-value	Distance to *mimp1* (bp)
21(M24)[a]	695	*Fo* solo LTR *Han* (AF076629)	3.10^{-94}	8
144(M24)[a]	331	*Fo* solo LTR *Han* (AF076629)	2.10^{-75}	3
104(MK)[a]	1403	*Fo* solo LTR *Han* (AF076629)	3.10^{-81}	578
109(Fh)[a]	762	*Nh PiggyBac*-like partial transposase [initially referred to as pathogenicity protein PEP1 (AAK18805)]	6.10^{-27}	277 (5′)
		Fg hypothetical protein FG05946	7.10^{-20}	
119(Fh)[a]	1023	*Fo mimp1* (AF76624)	8.10^{-13}	38
168(Fh)[a]	480	*Fo mimp1* (AF76624)	2.10^{-80}	2
		Fo impalaD (AF363425)	3.10^{-95}	79
Mimp1-9(L15)[a]	682	*Fo mimp1* (AF76624)	0.004	340
		Fo clone ACQ2_T7 transposon *impala* (AF285757)	0.0015	244
26(R4)[a]	1131	*Fg* hypothetical protein FG03406 (EAA71224)	6.10^{-26}	135 (5′)
		An pectin methylesterase (BAA75474)	3.10^{-11}	135 (5′)
18(*Fo5*)[b]	1800 (1185)	*Fg* hypothetical protein FG05987 (EAA75632)	2.10^{-31}	569 (5′)
		At phosphoglycerate/biphosphoglycerate mutase protein (NP_187168)	2.10^{-8}	569 (5′)
		Pc WRKY transcription factor (AAD55974)	0.001	ORF
25(*Fo5*)[b]	1502	*Fg* hypothetical protein FG00406 (EAA67497)	2.10^{-45}	294 (5′)
100(*Fo5*)[b]	3500 (1486 + 127)	*Fg* hypothetical protein FG01165 (EAA68631);	7.10^{-42}	277 (3′)
		St DNA mismatch repair protein (AAK58517)	0.023	>2000 (3′)
111H(*Fo5*)[b]	2800 (1080)	*Fg* hypothetical protein FG06828 (EAA76760)	7.10^{-20}	>1000 (5′)
		Sp MutS protein homolog 1 (O13921)	4.10^{-4}	>1000 (5′)
112(*Fo5*)[b]	1861	*Fg* hypothetical protein FG06184 (EAA74540)	3.10^{-60}	>1000 (5′)
		Ac Δ9-fatty acid desaturase (CAA59939)	7.10^{-29}	>1000 (5′)
120(*Fo5*)[b]	1500 (890)	*Fg* hypothetical protein FG10674 (EAA70296)	2.10^{-31}	125 (5′)
		Nc transcriptional factor PRO1 (XP_327678)	1.10^{-3}	125 (5′)

If sequence information was not obtained for the whole IPCR product, the size of the sequenced region is indicated in parentheses. BlastN or BlastX algorithms (Altschul *et al.* 1997) were used to search for significant matches in the databases. When a putative ORF was detected, the relative *mimp1* location was indicated as follows: 5′, 3′, and ORF indicate positions (nt) within the 5′ region, 3′ region, or the coding sequence of the putative gene, respectively. In such a case, two matches are listed for each alignment: the one giving the highest *e*-value and, when available, the first one giving information about gene function. *Fo, F. oxysporum*; *Fg, F. graminearum*; *Fh, F. hostae*; *An, Aspergillus niger*; *Nh, Nectria haematococca*; *At, Arabidopsis thaliana*; *Pc, Petroselinum crispum*; *St, Streptococcus thermophilus*; *Sp, Schizosaccharomyces pombe*; *Ac, Ajellomyces capsulatus*; *Nc, N. crassa.*

[a] Resident *mimp1* copies.

[b] Newly reinserted *mimp1* copies.

codon (Table 2). It is interesting to note that in three cases *mimp1* was found close to *F. oxysporum* solo-LTR *Han* or *Han*-like elements, which have a strong potential to form stable secondary structures (ΔG_0 values of −70 and −55 kcal/mol, respectively).

Sequence analysis of genomic regions flanking newly inserted *mimp1* in the FO5 background revealed a rather different situation. Of 13 reinsertion events, 7 did not show any significant matches, even when BLASTed against fungal-specific databases. The remaining 6 flanking regions all showed significant matches to known coding sequences (Table 2). In four revertants (18, 25, 100, and 120), insertion events occurred in close vicinity of open reading frames (ORFs) (Table 2). In revertant 120, for example, *mimp1* reinserted 125 bp upstream from an ORF encoding a putative Zn(2)Cys6 fungal transcription factor. Analysis of *mimp1* reinsertion sites in the *F. graminearum* genomic background was greatly facilitated by the availability of the genome sequence. First, flanking sequences were recovered by a modified TAIL–PCR procedure, easier to set up than IPCR, and second, the reinsertion sites could all be located at the nucleotide level by alignment with the genome sequence at MIPS (http://mips.gsf.de/genre/proj/fusarium/). The data obtained from the analysis of 12 reinsertion sites are of particular interest. Indeed, as shown in Table 3, in seven strains (58%), *mimp1* has reinserted <500 bp from a gene, a very promising result for use of *mimp1* as a tool for insertional mutagenesis.

DISCUSSION

Similarities between *impala* and *mimp1* TIRs and TSD, which are key components for the transposition reactions of many class II elements, led us to hypothesize a functional relationship between these two elements.

By analyzing the distribution of *impala* and *mimp1* elements across the Fusarium genus, we observed that

TABLE 3

Insertion sites of newly reinserted *mimp1* elements in the *F. graminearum* genetic context

Clone	*F. graminearum* contig DNA giving BLASTN hit[a]	Closest gene[b]	Distance to *mimp1* (bp)
1/6-1	1.450 (82,393)	FG10800	1025 (3′)
1/6l	1.415 (76,938)	FG09992	19 (5′)
1/6m	1.107 (33,781)	FG01974	115 (3′)
1/6n	1.193 (156,744)	FG04610	341 (5′)
1/12-1	1.298 (37,311)	FG07090	91 (5′)
1/12a	1.367 (81,420)	fgd367-380	675 (5′)
1/12d	1.40 (5,392)	FG00905	ORF
1/12e	1.74 (44,890)	FG01453	606 (3′)
1/24-1	1.293 (61,535)	fgd293-250	56 (5′)
1/24j	1.207 (94,644)	fgd207-380	214 (5′)
1/24k	1.294 (33,844)	FG07062	865 (5′)
5/19-1	1.254 (76,853)	FG06328	592 (5′)

The BlastN algorithm (Altschul *et al.* 1997) was used to search for significant matches in the *F. graminearum* genome database at MIPS (http://mips.gsf.de/genre/proj/fusarium/).

[a] Contig DNA from the *F. graminearum* genome sequence giving a hit with *mimp1* flanking sequences. The location of *mimp1* insertion in each contig DNA is indicated in parentheses. To determine the distance of *mimp1* reinsertion sites to genes, the annotated version of the *F. graminearum* genome sequence available at MIPS (http://mips.gsf.de/genre/proj/fusarium/) was used.

[b] The gene closest to the *mimp1* insertion site. The relative *mimp1* location was indicated as follows: 5′, 3′, and ORF indicate positions (nt) within the 5′ region, 3′ region, or the coding sequence of the gene, respectively.

both are widely distributed within the FOC complex, being present in closely related species and absent in more distantly related ones. The structural analysis of the *mimp1* family revealed a size homogeneity but a nucleotide divergence ranging from 0 to 20%, suggesting an old, but nevertheless recently active, element.

Overall, *mimp1* presented several features of MITEs except that its copy number appears unusually low. Indeed, most MITEs families in plant and animal species are associated with a high copy number (Tu 1997; Santiago *et al.* 2002), although rare examples of MITE families with moderate copy number have also been described (Holyoake and Kidwell 2003; Saito *et al.* 2005). The low copy number of *mimp1* could simply reflect the low activity of *impala*. This element itself is usually present in low copy number. Moreover, it is the representative of a basal branch of Tc1-like elements containing few members (Plasterk *et al.* 1999). On the other hand, as for all fungal genomes, the genome of *F. oxysporum*, estimated to be in the range of 40–50 Mb (Davière *et al.* 2001), is very small compared to genomes in which MITEs were found in large copy numbers. Considering that the larger the genome, the higher the number of transposable elements (Kidwell and Lisch 2002), huge amounts of TEs are not expected. This is supported by data from recently sequenced fungal genomes and other studies that reported a moderate TE content ~5–10% (Dean *et al.* 2005; Loftus *et al.* 2005) with a maximum of 20% for *Neurospora crassa* (Galagan *et al.* 2003). Finally, although a great diversity of TEs can be found (for review see Daboussi and Capy 2003), few MITE families have been identified in fungi up to now, suggesting that this kind of element is not very successful in such organisms.

Although a clear relationship between *mimp1* and *impala* was found, the origin of *mimp1* remains enigmatic. The simplest hypothesis is that *mimp1* was derived from *impala* by internal deletion. This is the case for *guest*, identified as a severely deleted relic of a full-length element in *N. crassa* (Ramussen *et al.* 2004). Several deletion derivatives of *impala* were identified (Hua-Van *et al.* 2001a; this work) and could always be unambiguously related to a particular *impala* subfamily due to the few nucleotide differences observed. The situation for *mimp1* is clearly different since no homology is detectable between *mimp1* and any of the *impala* subfamilies, except for the TIRs, implying a high selective pressure on these sequences. A *de novo* formation is also possible. This model supposes that new transposons can be created following the fortuitous association of TIRs bordering a segment of genomic DNA. This scenario was proposed for the origin of *Ds1* (MacRae and Clegg 1992) and the creation a new *P* element in Drosophila (Tsubota and Huong 1991).

Other *mimp* families with elements of the same size, exhibiting *impala*-like TIRs but with unrelated central regions, have been identified. Their analysis may help to clarify the origin of these elements.

In this study, we provide direct evidence that *impala* is the autonomous partner of *mimp1* since transposition of *mimp1* occurs only when a source of *impala* transposase is provided. The use of another genetic background

free of active *impala* elements (H. C. Kistler, personal communication), *F. graminearum*, confirmed the functional relationship between *mimp1* and *impala*. Although several MITE families could be linked to elements encoding a transposase on the basis of TIRs similarities (Jiang *et al.* 2003; Saito *et al.* 2005) and comobilization or *in vitro* physical interactions between the two suspected partners (Feschotte *et al.* 2005; Shan *et al.* 2005), there are very few cases of direct evidence of the mobilization of a MITE by an autonomous candidate (Rezsohazy *et al.* 1997; Jiang *et al.* 2003; Saito *et al.* 2005). The results presented here clearly connect a fungal MITE and the transposase of a *Tc1*-like element. This is the first functional system reported in fungi and a new example of a *Tc1/mariner*-related MITE.

We also show that *mimp1* transposes by a cut-and-paste mechanism. The transposition mechanism of MITEs has long remained mysterious because excision was rarely observed (Wessler *et al.* 1995; Wessler 1998). Direct evidence of excision was obtained recently with the rice element *mPing* (Kikuchi *et al.* 2003), allowing the classification of MITEs as class II elements. Our results reinforce the fact that MITEs are capable of both excision and reinsertion.

The characteristics of *impala* transposition, excision/reinsertion, excision footprints, and target-site duplication are retrieved for *mimp1*. It is noteworthy that interesting transposition specificities appeared associated to *mimp1*. First, the frequency of *mimp1* reinsertion, >80%, appears higher than that observed for *impala*. Second, one-third of the newly reinserted *mimp1* elements in *F. oxysporum* lie <500 nt from an ORF. Even more promising results were obtained in the *F. graminearum* strain as more than half of the reinsertion sites were shown to be located <500 nt from an ORF. The discrepancy between the two results might be due to differences between the two genomes but may also be attributed to the poor sequence availability in *F. oxysporum*.

Previous studies have demonstrated that MITEs are frequently found flanking many plant genes. *Tourist* and *Stowaway* have been identified in association with >100 plant genes (Bureau and Wessler 1992, 1994a,b). A computer-based systematic survey reveals a predominance of MITEs in wild-type rice genes (Bureau *et al.* 1996). However, the association of MITEs with genes is not uniform among the different MITE families, *i.e.*, only 10.5% for *explorer*, but nearly 98% for *Stowaway* (Mao *et al.* 2000). Some MITEs were found to insert into other MITEs or adjacent to other TEs (Jiang and Wessler 2001). This is what we observed in backgrounds containing TEs where *mimp1* insertions were frequently found within or adjacent to solo-LTRs, *mimp*, or *impala* elements but not to DNA transposons such as *Fot1* and *Hop* (Daboussi *et al.* 1992; Chalvet *et al.* 2003), although these elements constitute a much larger fraction of the genome. One explanation could be that *mimp1* amplification preceded the amplification of the TEs now found in a high copy number. Other hypotheses include preference for self-insertions or targeting through secondary structure, as proposed by Jiang and Wessler (2001). The fact that *Han*, *Han*-like, and *mimp* elements all can be folded into a stable secondary structure favors this hypothesis. The difference observed between resident and newly inserted copies may result from the differential richness of the TEs or may reflect the effect of selection on ancient insertions.

In conclusion, the identification of this mobilizing MITE system offers great prospects to tag genes in filamentous fungi. First, as for the *impala* system, the double component *mimp1/impala* is expected to function in a large range of fungal species. Second, if the higher ability to reinsert in the vicinity of genes is confirmed on a larger set of revertants, this system should represent a powerful molecular tool for the functional analysis of fungal genomes.

We thank Thomas Ruby, Gilles Pinto, and Corentin Laulier for their contributions to some experiments. This work was supported by grants from the Centre National de la Recherche Scientifique (CNRS) and Groupement de Recherche CNRS no. 2157 "Evolution des Eléments Transposables: du Gène aux Populations."

LITERATURE CITED

Altschul, S. F., T. L. Madden, A. A. Schäffer, J. Zhang, Z. Zhang *et al.*, 1997 Gapped BLAST and PSI-BLAST: a new generation of protein database search programs. Nucleic Acids Res. **25:** 3389–3402.

Baayen, R. P., K. O'Donnell, S. Breeuwsma, D. M. Geise and C. Waalwijk, 2001 Molecular relationships of fungi within the *Fusarium redolens-F. hostae* clade. Phytopathology **91:** 1037–1044.

Bureau, T. E., and S. R. Wessler, 1992 Tourist: a large family of small inverted repeat elements frequently associated with maize genes. Plant Cell **4:** 1283–1294.

Bureau, T. E., and S. R. Wessler, 1994a Mobile inverted-repeat elements of the *Tourist* family are associated with the genes of many cereal grasses. Proc. Natl. Acad. Sci. USA **91:** 1411–1415.

Bureau, T. E., and S. R. Wessler, 1994b *Stowaway*: a new family of inverted repeat elements associated with the genes of both monocotyledonous and dicotyledonous plants. Plant Cell **6:** 907–916.

Bureau, T. E., P. C. Ronald and S. R. Wessler, 1996 A computer-based systematic survey reveals the predominance of small inverted-repeat elements in wild-type rice genes. Proc. Natl. Acad. Sci. USA **93:** 8524–8529.

Carroll, A. M. C., J. A. Sweigard and B. Valent, 1994 Improved vectors for selecting resistance to hygromycin. Fungal Genet. Newsl. **41:** 22.

Casacuberta, E., J. M. Casacuberta, P. Puigdomenech and A. Monfort, 1998 Presence of miniature inverted-repeat transposable elements (MITEs) in the genome of *Arabidopsis thaliana*: characterisation of the *Emigrant* family of elements. Plant J. **16:** 79–85.

Chalvet, F., C. Grimaldi, F. Kaper, T. Langin and M. J. Daboussi, 2003 *Hop*, an active *Mutator*-like element in the genome of the fungus *Fusarium oxysporum*. Mol. Biol. Evol. **20:** 1362–1375.

Daboussi, M., and P. Capy, 2003 Transposable elements in filamentous fungi. Annu. Rev. Microbiol. **57:** 275–299.

Daboussi, M. J., and T. Langin, 1994 Transposable elements in the fungal plant pathogen *Fusarium oxysporum*. Genetica **93:** 49–59.

Daboussi, M. J., T. Langin and Y. Brygoo, 1992 *Fot1*, a new family of fungal transposable elements. Mol. Gen. Genet. **232:** 12–16.

Daboussi, M. J., J. M. Davière, S. Graziani and T. Langin, 2002 Evolution of the *Fot1* transposons in the genus *Fusarium*: discontinuous distribution and epigenetic inactivation. Mol. Biol. Evol. **19:** 510–520.

Davière, J. M., T. Langin and M. J. Daboussi, 2001 Potential role of transposable elements in the rapid reorganization of the *Fusarium oxysporum* genome. Fungal Genet. Biol. **34:** 177–192.

Dean, R. A., N. J. Talbot, D. J. Ebbole, M. L. Farman, T. K. Mitchell *et al.*, 2005 The genome sequence of the rice blast fungus *Magnaporthe grisea*. Nature **434:** 980–986.

Feschotte, C., and C. Mouches, 2000 Evidence that a family of miniature inverted-repeat transposable elements (MITEs) from the *Arabidopsis thaliana* genome has arisen from a *pogo*-like DNA transposon. Mol. Biol. Evol. **17:** 730–737.

Feschotte, C., X. Zhang and S. R. Wessler, 2002 Miniature inverted-repeat transposable elements and their relationship to established DNA transposons, pp. 1147–1158 in *Mobile DNA II*, edited by N. L. Craig, R. Craigie, M. Gellert and A. M. Lambowitz. American Society of Microbiology, Washington, DC.

Feschotte, C., M. T. Osterlund, R. Peeler and S. R. Wessler, 2005 DNA-binding specificity of rice mariner-like transposases and interactions with *Stowaway* MITEs. Nucleic Acids Res. **33:** 2153–2165.

Galagan, J. E., S. E. Calvo, K. A. Borkovich, E. U. Selker, N. D. Read *et al.*, 2003 The genome sequence of the filamentous fungus *Neurospora crassa*. Nature **422:** 859–868.

Holyoake, A. J., and M. G. Kidwell, 2003 Vege and Mar: two novel hAT MITE families from Drosophila willistoni. Mol. Biol. Evol. **20:** 163–167.

Hua-Van, A., F. Héricourt, P. Capy, M. J. Daboussi and T. Langin, 1998 Three highly divergent subfamilies of the *impala* transposable element coexist in the genome of the fungus *Fusarium oxysporum*. Mol. Gen. Genet. **259:** 354–362.

Hua-Van, A., J. M. Davière, T. Langin and M. J. Daboussi, 2000 Genome organization in *Fusarium oxysporum*: clusters of class II transposons. Curr. Genet. **37:** 339–347.

Hua-Van, A., T. Langin and M. J. Daboussi, 2001a Evolutionary history of the *impala* transposon in *Fusarium oxysporum*. Mol. Biol. Evol. **18:** 1959–1969.

Hua-Van, A., J. A. Pamphile, T. Langin and M. J. Daboussi, 2001b Transposition of autonomous and engineered *impala* transposons in *Fusarium oxysporum* and a related species. Mol. Gen. Genet. **264:** 724–731.

Jiang, N., and S. R. Wessler, 2001 Insertion preference of maize and rice miniature inverted repeat transposable elements as revealed by the analysis of nested elements. Plant Cell **13:** 2553–2564.

Jiang, N., Z. Bao, X. Zhang, H. Hirochika, S. R. Eddy *et al.*, 2003 An active DNA transposon family in rice. Nature **421:** 163–167.

Kidwell, M. G., and D. R. Lisch, 2002 Transposable elements as sources of genomic variation, pp. 59–90 in *Mobile DNA II*, edited by N. L. Craig, R. Craigie, M. Gellert and A. M. Lambowitz. American Society of Microbiology, Washington, DC.

Kikuchi, K., K. Terauchi, M. Wada and H. Y. Hirano, 2003 The plant MITE *mPing* is mobilized in anther culture. Nature **421:** 167–170.

Kunze, R., and C. F. Weil, 2002 The *hAT* and CACTA superfamilies of plant transposons, pp. 565–610 in *Mobile DNA II*, edited by N. L. Craig, R. Craigie, M. Gellert and A. M. Lambowitz. American Society of Microbiology, Washington, DC.

Langin, T., M. J. Daboussi, C. Gerlinger and Y. Brygoo, 1990 Influence of biological parameters and gene transfer technique on transformation of *Fusarium oxysporum*. Curr. Genet. **17:** 313–319.

Li Destri Nicosia, M. G., C. Brocard-Masson, S. Demais, A. Hua Van, M. J. Daboussi *et al.*, 2001 Heterologous transposition in *Aspergillus nidulans*. Mol. Microbiol. **39:** 1330–1344.

Liu, Y. G., and R. F. Whittier, 1995 Thermal asymmetric interlaced PCR: automatable amplification and sequencing of insert end fragments from P1 and YAC clones for chromosome walking. Genomics **25:** 674–681.

Loftus, B. J., E. Fung, P. Roncaglia, D. Rowley, P. Amedeo *et al.*, 2005 The genome of the basidiomycetous yeast and human pathogen *Cryptococcus neoformans*. Science **307:** 1321–1324.

MacRae, A. F., and M. T. Clegg, 1992 Evolution of *Ac* and *Dsl* elements in select grasses (Poaceae). Genetica **86:** 55–66.

Malardier, L., M. J. Daboussi, J. Julien, F. Roussel, C. Scazzocchio *et al.*, 1989 Cloning of the nitrate reductase gene (*niaD*) of *Aspergillus nidulans* and its use for transformation of *Fusarium oxysporum*. Gene **78:** 147–156.

Mao, L., T. C. Wood, Y. Yu, M. A. Budiman, J. Tomkins *et al.*, 2000 Rice transposable elements: a survey of 73,000 sequence-tagged-connectors. Genome Res. **10:** 982–990.

Migheli, Q., R. Lauge, J. M. Daviere, C. Gerlinger, F. Kaper *et al.*, 1999 Transposition of the autonomous *Fot1* element in the filamentous fungus *Fusarium oxysporum*. Genetics **151:** 1005–1013.

Migheli, Q., C. Steinberg, J. M. Davière, C. Olivain, C. Gerlinger *et al.*, 2000 Recovery of mutants impaired in pathogenicity after transposition of *Impala* in *Fusarium oxysporum* f. sp. *melonis*. Phytopathology **90:** 1279–1284.

Oosumi, T., B. Garlick and W. R. Belknap, 1996 Identification of putative nonautonomous transposable elements associated with several transposon families in *Caenorhabditis elegans*. J. Mol. Evol. **43:** 11–18.

Plasterk, R. H., Z. Izsvak and Z. Ivics, 1999 Resident aliens: the *Tc1/mariner* superfamily of transposable elements. Trends Genet. **15:** 326–332.

Punt, P. J., R. P. Oliver, M. A. Dingemanse, P. H. Pouwels and C. A. van den Hondel, 1987 Transformation of *Aspergillus* based on the hygromycin B resistance marker from *Escherichia coli*. Gene **56:** 117–124.

Ramussen, J. P., A. H. Taylor, L. J. Ma, S. Purcell, F. Kempken *et al.*, 2004 *Guest*, a transposable element belonging to the *Tc1/mariner* superfamily is an ancient invader of *Neurospora* genomes. Fungal Genet. Biol. **41:** 52–61.

Rezsohazy, R., H. G. van Luenen, R. M. Durbin and R. H. Plasterk, 1997 Tc7, a Tc1-hitch hiking transposon in Caenorhabditis elegans. Nucleic Acids Res. **25:** 4048–4054.

Robertson, H. M., 2002 Evolution of DNA transposons in eukaryotes, pp. 1093–1110 in *Mobile DNA II*, edited by N. L. Craig, R. Craigie, M. Gellert and A. M. Lambowitz. American Society of Microbiology Press, Washington, DC.

Saito, M., J. Yonemaru, G. Ishikawa and T. Nakamura, 2005 A candidate autonomous version of the wheat MITE *Hikkoshi* is present in the rice genome. Mol. Genet. Genomics **273:** 404–414.

Sambrook, J., E. F. Fritsch and T. Maniatis, 1989 *Molecular Cloning: A Laboratory Manual*, Ed. 2. Cold Spring Harbor Laboratory Press, Cold Spring Harbor, NY.

Santiago, N., C. Herraiz, J. R. Goni, X. Messeguer and J. M. Casacuberta, 2002 Genome-wide analysis of the *Emigrant* family of MITEs of *Arabidopsis thaliana*. Mol. Biol. Evol. **19:** 2285–2293.

Shan, X., Z. Liu, Z. Dong, Y. Wang, Y. Chen *et al.*, 2005 Mobilization of the active MITE transposons *mPing* and *Pong* in rice by introgression from wild rice (*Zizania latifolia* Griseb.). Mol. Biol. Evol. **22:** 976–990.

Skovgaard, K., S. Rosendahl, K. O'Donnell and H. I. Nirenberg, 2003 *Fusarium commune* is a new species identified by morphological and molecular phylogenetic data. Mycologia **95:** 630–636.

Smit, A. F., and A. D. Riggs, 1996 Tiggers and DNA transposon fossils in the human genome. Proc. Natl. Acad. Sci. USA **93:** 1443–1448.

Swofford, D. L., 2002 *PAUP*: Phylogenetic Analysis Using Parsimony (*and Other Methods)*. Sinauer Associates, Sunderland, MA.

Thompson, J. D., D. G. Higgins and T. J. Gibson, 1994 CLUSTAL W: improving the sensitivity of progressive multiple sequence alignment through sequence weighting, positions-specific gap penalties and weight matrix choice. Nucleic Acids Res. **22:** 4673–4680.

Tsubota, S. I., and D. V. Huong, 1991 Capture of flanking DNA by a P element in Drosophila melanogaster: creation of a transposable element. Proc. Natl. Acad. Sci. USA **88:** 693–697.

Tu, Z., 1997 Three novel families of miniature inverted-repeat transposable elements are associated with genes of the yellow fever mosquito, *Aedes aegypti*. Proc. Natl. Acad. Sci. USA **94:** 7475–7480.

Tu, Z., 2001 Eight novel families of miniature inverted repeat transposable elements in the African malaria mosquito, *Anopheles gambiae*. Proc. Natl. Acad. Sci. USA **98:** 1699–1704.

Wessler, S., 1998 Transposable elements associated with normal plant genes. Physiol. Plant **103:** 581–583.

Wessler, S. R., T. E. Bureau and S. E. White, 1995 LTR-retrotransposons and MITEs: important players in the evolution of plant genomes. Curr. Opin. Genet. Dev. **5:** 814–821.

Yeadon, P. J., and D. E. Catcheside, 1995 *Guest*: a 98 bp inverted repeat transposable element in *Neurospora crassa*. Mol. Gen. Genet. **247:** 105–109.

Zhang, Q., J. Arbuckle and S. R. Wessler, 2000 Recent, extensive, and preferential insertion of members of the miniature inverted-repeat transposable element family *Heartbreaker* into genic regions of maize. Proc. Natl. Acad. Sci. USA **97:** 1160–1165.

Zhang, X., C. Feschotte, Q. Zhang, N. Jiang, W. B. Eggleston *et al.*, 2001 P instability factor: an active maize transposon system associated with the amplification of *Tourist*-like MITEs and a new superfamily of transposases. Proc. Natl. Acad. Sci. USA **98:** 12572–12577.

Communicating editor: D. Voytas